JCAMECH

Vol. 51, No. 2, December 2020, pp 332-339
DOI: 10.22059/jcamech.2019.293933.460

Thermoelastic response of microbeams under a magnetic field rested on two-parameter viscoelastic foundation

Adam Zakria [a,b*] and Ahmed E. Abouelregal [a,c]

[a] *Department of Mathematics, College of Science and Arts, Jouf University, Qurayyat, Saudi Arabia*
[b] *Faculty of Science, Department of Mathematics, University of Kordofan, Sudan*
[c] *Department of Mathematics, Faculty of Science, Mansoura University, Mansoura 35516, Egypt,*

ARTICLE INFO

Article history:
Received 12 December 2019
Accepted 27 December 2019

Keywords:
Microbeams
Thermoelasticity
Magnetic field
Pasternak foundation
Phase lags

ABSTRACT

Mechanical foundations and pavement design need a perfect prediction of the response of the material to reach a reliable and safe structure. This work deals with the thermoelastic response of microbeams rested on a two-parameter viscoelastic foundation due to a magnetic field in the context of the dual-phase lag thermoelasticity model. The solutions of the governing equations are attained using the Laplace transform method. The distributions of the deflection, temperature, displacement and the flexure moment of the microbeam are numerically obtained and illustrated graphically. The effects of the magnetic field, Winkler and shear foundation parameters, the ramping time parameter and the models of thermoelasticity on the considered fields are concerned and discussed in details. For comparison purposes, the response of the microbeam and the dynamic deflection using the Bernoulli-Euler beam and thermoelasticity theories are compared with earlier investigated studies and magnificent agreements are detected.

1. Introduction

Microbeams are very important in the applications of Micro-electro-mechanical systems (MEMS) and Nano-electro-mechanical systems (NEMS). The axial parameters of a microbeam are applied to cause changes in its distributive behaviors. These differences in distribution allow the use of a small beam as a sensor to measure physical quantities such as the deflection, the displacement, temperature and the flexure moment. In recent decades, the thermal response of microbeams has been studied and there are many interesting papers published in this area of research (see Akgöz and Civalek [1], Thai, et al. [2], Akgöz and Civalek [3], Belardinelli, et al. [4], Baghani [5]).

Recently, non-ideal boundary conditions have been investigated for both microbeams.Pakdemirli and Boyacı [6] studied the concept of boundary conditions to the microbeam problem. A linear and non-linear model of microbeam was introduced to investigate the initial resonance of the microbeam due to consistent external distributed force, and the effect of linear and non-linear foundation on the required vibration response is noted. These variations of conditions allow the use of

a micro-beam as a sensor to measure physical quantities such as the deflection, temperature, displacement and the flexure moment which are important to various kinds of research (Safarabadi, et al. [7], Baghani, et al. [8], Şimşek [9], Ghayesh, et al. [10], Caputo [11], El-Karamany and Ezzat [12]).

The highway pavements, railroad tracks, and strip foundations that take into account different types of foundations such as Pasternak, Winkler, flexible or sticky, are among the issues related to the interaction of soil structure. The problems of the physical fields of beams on continuous elastic foundations have been investigated by a number of researchers. For instance, the effect of sticky foundation on the deflection behaviors of mechanical and precision mechanics was sticky investigated by Pradhan and Murmu [13], Goodarzi, et al. [14], Mohammadi, et al. [15], Mohammadi, et al. [16], Younis, et al. [17], Zenkour and Sobhy [18]. Also, Chen, et al. [19] discussed the dynamic stiffness of the beams based on the viscosity due to harmonic motion. In addition, Abdalla and Ibrahim [20] used the discrete Reissner–Mindlin element to explain the problem of thin and thick plates resting on the Winkler-type foundation.

There is a growing interest in the generalized theory of thermoelasticity, which has been found to produce more realistic results than double or unplanned models of thermoelasticity, especially when short time effects or temperature gradients are considered. The thermoelastic diffusion theory that uses the thermal elastic model was developed by Kumar, et al. [21].Also,

* Corresponding author. E-mail: azsidig@ju.edu.sa

Tzou [22], Tzou [23] proposed a new concept of dual-phase-lag (DPL) model in which the heat flux and temperature gradient could be simulated with lag times. In addition, Biot [24] investigated the theory of the classical dynamical thermoelasticity (CTE).

This study is an effort to study a thermoelastic response of microbeams under various magnetic fields based on the DPL thermoelasticity model. Also, an important comparison between different models of thermoelasticity and their effect on different fields is illustrated. Non-dimensional variables with the analytical Laplace transform technique are used to compute the vibration of the studied fields of the microbeams. Some comparisons have been also shown graphically to estimate the effects of Winkler and shear foundation parameters, the magnetic field, phase lags and ramping time parameters on all the physical fields.

2. Formulation of the Problem

We consider a thermoelastic thin microbeam initially at temperature T_0 rested on a two-parameter viscoelastic foundation. A linear viscoelastic foundation model is shown in Fig. (a) where the foundation is modeled by introducing a shear layer mounted on a set of linear elastic springs. Let us consider that the x-axis is drawn along the axial tendency of the beam and y, z axes agree to the width and thickness, correspondingly. The teeny deflections of the microbeam with dimensions of length L, width b and thickness h and cross-section area $A = bh$ are considered.

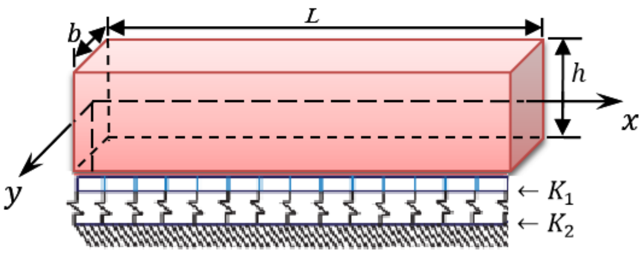

Fig. a. Schematic diagram for the microbeam.

According to Euler–Bernouilli beam theory, the components of displacement vector are given by:

$$u = -z\frac{\partial w}{\partial x}, v = 0, \ w(x, y, z, t) = w(x, t) \tag{1}$$

For a one-dimensional problem, the constitutive equation after using Eqs. (1) can be expressed as

$$\sigma_x = -E\left[\frac{\partial^2 w}{\partial x^2} + \alpha_T \theta\right] \tag{2}$$

Where σ_x is the nonlocal axial stress, and $\alpha_T = \alpha_t/(1-2\nu)$. With aid of Eq. (2), the flexure moment M is given by

$$M(x, t) = -IE\left[\frac{\partial^2 w}{\partial x^2} + \alpha_T M_T\right] \tag{3}$$

where

$$M_T = \frac{12}{h^3}\int_{-h/2}^{h/2} \theta(x, z, t) z dz \tag{4}$$

Due to the application of the initial magnetic field H and the density of the current J, there results an induced magnetic and electric fields h and E. The Maxwell's equations for a homogeneous and electrically perfect conducting thermoelastic solid (neglecting the charge density) can be recovered as Wang, et al. [25]

$$J = \nabla \times h, \ \ \nabla \times E = -\mu_0 \frac{\partial h}{\partial t}, \ \ \ E = -\mu_0\left(\frac{\partial u}{\partial t} \times H\right) \tag{5}$$
$$h = \nabla \times (u \times h), \ \ \nabla \cdot h = 0$$

We can write the vector of the induced magnetic field h and current density J as follows:

$$J = \nabla \times h, \ \ \nabla \times E = -\mu_0 \frac{\partial h}{\partial t}, \ \ \ E = -\mu_0\left(\frac{\partial u}{\partial t} \times H\right) \tag{6}$$
$$h = \nabla \times (u \times h), \ \ \nabla \cdot h = 0$$

Using previous equation (6) into the expressions for the Lorentz force F induced by the applying longitudinal magnetic field H, yields

$$F = (f_x, f_y, f_z) = \mu_0 H_x^2\left(0, 0, \frac{\partial^2 w}{\partial x^2}\right) \tag{7}$$

As is known, the Winkler model of the elastic foundation is the most preliminary in which the vertical displacement is assumed to be proportional to the contact pressure at an arbitrary point (see Hetenyi [26]). Due to the interaction between the microbeam and the supporting foundation, the normal stress per unit area R_f (foundation reaction) and vertical displacement w at an arbitrary point on the lower boundary of the microbeam holds the following relationship

$$R_f = K_w w(x, t) - K_s \frac{\partial^2 w(x,t)}{\partial x^2} \tag{8}$$

Where K_w is the Winkler's foundation modulus, and K_s is the shear foundation modulus. It is observed that when $K_s = 0$, Eq. (8) is equivalent to that of the microbeam on a Winkler foundation type; also, when $K_w = K_s = 0$ (the subgrade reactions are zero), indicating that the microbeam not have a foundation. The equation of motion for the transverse response of microbeams can be written as

$$\frac{\partial^2 M}{\partial x^2} - R_f + f(x) = \rho A \frac{\partial^2 w}{\partial t^2} \tag{9}$$

where $f(x)$ is a function of space to incorporate the longitudinal magnetic force. Here $f(x) \neq f_z$, since f_z is a body force and $f(x)$ denotes the force per length. So, $f(x)$ can be written as

$$f(x) = Af_z = A\mu_0 H_x^2 \frac{\partial^2 w}{\partial x^2} \tag{10}$$

Introducing Eqs. (3), (8) and (10) into Eq. (9), the following motion equation of the mirobeam is obtained

$$\frac{\partial^4 w}{\partial x^4} - \left(\frac{K_s}{IE} + \frac{A\mu_0 H_x^2}{IE}\right)\frac{\partial^2 w}{\partial x^2} + \frac{\rho A}{IE}\frac{\partial^2 w}{\partial t^2} + \frac{K_w}{IE} w + \alpha_T \frac{\partial^2 M_T}{\partial x^2} = 0 \tag{11}$$

The generalized heat conduction in the context of Tzou [22] theory is given by

$$K\left(1 + \tau_\theta \frac{\partial}{\partial t}\right)\left(\frac{\partial^2 \theta}{\partial x^2} + \frac{\partial^2 \theta}{\partial z^2}\right) = \left(1 + \tau_q \frac{\partial}{\partial t} + \frac{\tau_q^2}{2}\frac{\partial^2}{\partial t^2}\right)\left[\rho C_E \frac{\partial \theta}{\partial t} + \gamma T_0 \frac{\partial e}{\partial t}\right] \tag{12}$$

Putting Eq. (1) into (12), we get the generalized heat conduction equation as

$$\left(1 + \tau_\theta \frac{\partial}{\partial t}\right)\left(\frac{\partial^2 \theta}{\partial x^2} + \frac{\partial^2 \theta}{\partial z^2}\right) = \tag{13}$$
$$\left(1 + \tau_q \frac{\partial}{\partial t} + \frac{\tau_q^2}{2}\frac{\partial^2}{\partial t^2}\right)\left[\frac{\rho C_E}{K}\frac{\partial \theta}{\partial t} - \frac{\gamma T_0}{K} z \frac{\partial}{\partial t}\left(\frac{\partial^2 w}{\partial x^2}\right)\right]$$

3. Solution of the Problem

For a very thin microbeam, assuming that the increment temperature varies in a sinusoidal form along the thickness direction and also the microbeam is thermally insulated. Then, the variation of the temperature can be expressed as

$$\theta(x,z,t) = \Theta(x,t)\sin\left(\frac{\pi z}{h}\right) \tag{14}$$

Substituting Eq. (14) into Eq. (11), the motion equation (11) can be represented as

$$\frac{\partial^4 w}{\partial x^4} - \left(\frac{K_s}{IE} + \frac{A\mu_0 H_x^2}{IE}\right)\frac{\partial^2 w}{\partial x^2} + \frac{\rho A}{IE}\frac{\partial^2 w}{\partial t^2} + \frac{K_w}{IE}w + \frac{24\alpha_T}{h\pi^2}\frac{\partial^2 \Theta}{\partial x^2} = 0 \tag{15}$$

From Eqs. (3) and (14), the flexure moment M can be written as

$$M(x,t) = -IE\frac{\partial^2 w(x,t)}{\partial x^2} - \frac{24IE\alpha_T}{h\pi^2}\Theta \tag{16}$$

Integrating Eq. (13) with respect to z through the thickness of the microbeam from $\frac{-h}{2}$ to $\frac{h}{2}$, yields

$$\begin{gathered}\left(1+\tau_\theta\frac{\partial}{\partial t}\right)\left(\frac{\partial^2}{\partial x^2} - \frac{\pi^2}{h^2}\right)\Theta = \\ \left(1+\tau_q\frac{\partial}{\partial t} + \frac{\tau_q^2}{2}\frac{\partial^2}{\partial t^2}\right)\left[\frac{1}{k}\frac{\partial\Theta}{\partial t} - \frac{\gamma T_0\pi^2 h}{K}\frac{\partial}{\partial t}\left(\frac{\partial^2 w}{\partial x^2}\right)\right]\end{gathered} \tag{17}$$

To facilitate the numerical analysis, the following dimensionless parameters are introduced:

$$\begin{gathered}\{x', z', u', w'\} = \frac{1}{L}\{x, z, u, w\},\quad \{t', \tau'_q\} = \frac{c_0}{L}\{t, \tau_q\},\\ \Theta' = \frac{\Theta}{T_0},\quad \sigma'_x = \frac{\sigma_x}{E},\quad M' = \frac{M}{ALE},\quad c_0 = \sqrt{\frac{E}{\rho}}.\end{gathered} \tag{18}$$

So, the basic equations in nondimensional forms are simplified as

$$\begin{gathered}\frac{\partial^4 w}{\partial x^4} - A_1\frac{\partial^2 w}{\partial x^2} + A_2\frac{\partial^2 w}{\partial t^2} + A_3 w = -A_4\frac{\partial^2 \Theta}{\partial x^2}\\ \left(1+\tau_\theta\frac{\partial}{\partial t}\right)\left(\frac{\partial^2}{\partial x^2} - A_5\right)\Theta = \left(1+\tau_q\frac{\partial}{\partial t} + \frac{\tau_q^2}{2}\frac{\partial^2}{\partial t^2}\right)\left[A_6\frac{\partial\Theta}{\partial t} - A_7\frac{\partial}{\partial t}\left(\frac{\partial^2 w}{\partial x^2}\right)\right]\end{gathered} \tag{19}$$

$$M(x,t) = -A_8\frac{\partial^2 w(x,t)}{\partial x^2} - A_9\Theta \tag{20}$$

where

$$A_1 = L^2\left(\frac{12K_s}{h^3 bE} + \frac{12\mu_0 H_x^2}{h^2 E}\right),\ A_2 = \frac{12L^2}{h^2},\ A_3 = \frac{12L^4 K_w}{bh^3 E},\ A_4 = \frac{24LT_0\alpha_T}{h\pi^2},$$

$$A_5 = \frac{L^2\pi^2}{h^2},\ A_6 = \frac{L}{k}\sqrt{\frac{E}{\rho}},\ A_7 = \frac{\gamma\pi^2 h}{24K}\sqrt{\frac{E}{\rho}},\ A_8 = \frac{h^2}{12bL^2},\ A_9 = \frac{2hT_0\alpha_T}{L\pi^2}.$$

4. Initial and boundary conditions

To solve the problem, the initial and boundary conditions essential be reserved into consideration. The homogeneous initial conditions are reserved as

$$\Theta(x,0) = \frac{\partial\Theta(x,0)}{\partial t} = 0 = w(x,0) = \frac{\partial w(x,0)}{\partial t} \tag{21}$$

For example, we'll assume that both ends of the mirobeam satisfy

$$w(0,t) = w(L,t) = 0 = \frac{\partial^2 w(0,t)}{\partial x^2} = \frac{\partial^2 w(L,t)}{\partial x^2} \tag{22}$$

Also, we assume that the mirobeam is loaded thermally by ramp-type heating , hence

$$\Theta(x,t) = \Theta_0\begin{cases}0, & t \le 0\\ \frac{t}{t_0}, & 0 \le t \le t_0\\ 1, & t > 0\end{cases} \tag{23}$$

wherever t_0 is ramp-type parameter and Θ_0 is a constant. Moreover, the temperature at the end boundary should achieve the following relationship

$$\frac{\partial\Theta}{\partial x} = 0 \quad \text{on} \quad x = L \tag{24}$$

5. Solution of the problem in the Laplace transform domain

Using the Laplace transform defined by

$$\bar{f}(x,t) = \int_0^\infty f(x,t)e^{-st}dt \tag{25}$$

to both sides of Eqs. (19) and (20) and by the homogeneous initial conditions (21), one gets the field equations in the Laplace transform space as

$$\begin{gathered}\frac{d^4\bar{w}}{dx^4} - A_{10}\frac{d^2\bar{w}}{dx^2} + A_{11}\bar{w} = -A_{12}\frac{d^2\bar{\Theta}}{dx^2}\\ \left(\frac{d^2}{dx^2} - A_{13}\right)\bar{\Theta} = -A_{14}\frac{d^2\bar{w}}{dx^2}\end{gathered} \tag{26}$$

$$\bar{M}(x,s) = -A_{15}\frac{d^2\bar{w}}{dx^2} - A_{16}\bar{\Theta} \tag{27}$$

where

$$A_{11} = s^2 A_2 + A_3,\ A_{12} = A_4,\ A_{13} = A_5 + A_6\frac{(s + s^2\tau_q + s^3\tau_q^2)}{(1+\tau_\theta s)}$$

$$A_{10} = A_1,\ A_{14} = A_7\frac{(s + s^2\tau_q + s^3\tau_q^2)}{(1+\tau_\theta s)},\ A_{15} = A_8,\ A_{16} = A_9.$$

Elimination Θ or $\bar{w}$ from Eqs. (26), one obtains:

$$(D^6 - AD^4 + BD^2 - C)\{\bar{w}, \bar{\Theta}\}(x) = 0 \tag{28}$$

where A, B and C are given in (29)

$$\begin{gathered}A = A_{10} + A_{14} + A_{12}A_{14},\ B = A_{10}A_{14} + A_{11},\\ C = A_{11}A_{14},\ D = \frac{d}{dx}\end{gathered} \tag{29}$$

Equation (28) can be moderated to

$$(D^2 - m_1^2)(D^2 - m_2^2)(D^2 - m_3^2)\{\bar{w}, \bar{\Theta}\}(x) = 0 \tag{30}$$

where $m_n^2, n = 1,2,3,4$ are roots of

$$m^6 - Am^4 + Bm^2 - C = 0 \tag{31}$$

The solution of equation (31) in the Laplace transformation domain can be characterized as

$$\{\bar{w}, \bar{\Theta}\}(x) = \sum_{n=1}^{3}\left(\{1, \beta_n\}C_n e^{-m_n x} + \{1, \beta_{n+3}\}C_{n+3}e^{m_n x}\right) \tag{32}$$

Where the consensus between these two equations and Eq. (27), we get

$$\beta_n = -\frac{m_n^2 A_{14}}{m_n^2 - A_{13}} \tag{33}$$

The displacement can be obtained after using Eq. (32) as follows

$$\bar{u}(x) = -z\frac{d\bar{w}}{dx} = z\sum_{n=1}^{3} m_n\left(C_n e^{-m_n x} - C_{n+3}e^{m_n x}\right) \tag{34}$$

Substituting the expressions of $\bar{w}$ and Θ from (32) into (28), we got to solve the flexure moment M as follows:

$$\bar{M}(x) = -\sum_{n=1}^{3}\left(m_n^2 A_{15} + A_{16}\beta_n\right)\left(C_n e^{-m_n x} + C_{n+3}e^{m_n x}\right) \tag{35}$$

Also, the strain gives

$$\bar{e}(x) = \frac{d\bar{u}}{dx} = -z\sum_{n=1}^{3} m_n^2\left(C_n e^{-m_n x} + C_{n+1}e^{m_n x}\right) \tag{36}$$

After applying Laplace transform, the boundary conditions (21)-(23) take the forms

$$\begin{gathered}
\bar{w}(0,s) = \bar{w}(L,s) = 0 \\
\frac{\partial^2\bar{w}(0,s)}{\partial x^2} = \frac{\partial^2\bar{w}(L,s)}{\partial x^2} = 0 \\
\frac{\partial\bar{\Theta}(0,s)}{\partial x} = \Theta_0\left(\frac{1-e^{-st_0}}{s^2 t_0}\right) = \bar{G}(s) \\
\frac{\partial\bar{\Theta}(L,s)}{\partial x} = 0
\end{gathered} \tag{37}$$

Replacing Eq. (32) in the above-mentioned boundary conditions, one obtains six linear equations

$$\begin{gathered}
\sum_{n=1}^{3}\left(C_n + C_{n+1}\right) = 0, \\
\sum_{n=1}^{3}\left(C_n e^{-m_n L} + C_{n+1}e^{m_n L}\right) = 0
\end{gathered} \tag{38}$$

$$\begin{gathered}
\sum_{n=1}^{3} m_n^2\left(C_n + C_{n+1}\right) = 0 \\
\sum_{n=1}^{3} m_n^2\left(C_n e^{-m_n L} + C_{n+1}e^{m_n L}\right) = 0
\end{gathered} \tag{39}$$

$$\begin{gathered}
\sum_{n=1}^{3} m_n\left(\beta_n C_n - \beta_{n+1}C_{n+1}\right) = -\mathrm{G}(s) \\
\sum_{n=1}^{3} m_n\left(\beta_n C_n e^{-m_n L} - \beta_{n+1}C_{n+1}e^{m_n L}\right) = 0
\end{gathered} \tag{40}$$

The solution to the system of linear equations above provides unknown parameters C_n, $(n = 1,2,\ldots,6)$. To determine the fields studied in the physical field, a Riemann sum approximation method is used to obtain numerical results.

6. Numerical results

Using the theoretical analysis described in the previous sections, and to assess the effects Winkler and shear foundation parameters K_w and K_s , initial magnetic field H_x and ramping time parameter t_0 on the deflection w , temperature θ , displacement u and the flexure moment M distributions, a marginal study is conducted as follows. A comparison of our results with those of other articles can be seen in Figs. 1-16. The physical and geometrical properties of the microbeam are listed in Table 1. Numerical calculations and graphs have been divided into four cases.

Table1: Mechanical and thermoelastic properties of the microbeam ($T_0 = 293\mathrm{K}$) :

Material properties	Value
Thermal conductivity K ($\mathrm{W\,m^{-1}K^{-1}}$)	156
Young' modulus E (GPa)	169
Density ρ ($\mathrm{Kgm^{-3}}$)	2330
Thermal expansion α_t ($\mathrm{K^{-1}}$)	2.59×10^{-6}
Thermal diffusivity k ($\mathrm{m^2s^{-1}}$)	9.4×10^{-5}
Poisson's ratio ν	0.22
Specific heat C_E (J/kgK)	713

6.1. *The effect of the initial magnetic field parameter*

In this case, we have studied the effect of the initial magnetic field parameter H_x on all studied field variables (w, θ, u, M) in the wide range $1 \leq x \leq 2$. We take the initial magnetic field $H_x = 10, 20, 30$ in the presence of the magnetic field and put the parameter $H_x = 0$ when the magnetic field is absent. The other parameters are assumed to be constants ($K_w = 100, K_s = 50, \tau_\theta = 0.05, \tau_q = 0.03$ and $t_0 = 0.1$). The results obtained are displayed graphically in Figs. 1-4. From Figs. (1−4) we can see that the parameter H_x has a great effect on all the studied fields. Also, we can observe that the deflection w start increasing with parameter H_x in the range$1 \leq x \leq 1.4$, thereafter decreasing in the range $1.4 \leq x \leq 2$. The natural temperature θ vs the magnetic field parameter is plotted in Fig. 2. We observed that the increase in the value of H_x causes an increase in the values of temperature θ . The variation of displacement u vs the distance is plotted in Fig. 3. From the figure, we observed that the increase in the value of the H_x causes decrease in the values of the displacement u . As seen in Fig. 4, it is to be noted that the flexure moment M start increases with parameter H_x in the wide range $1 \leq x \leq 1.1$, thereafter the profile decreasing on the interval $1.1 \leq x \leq 2$.

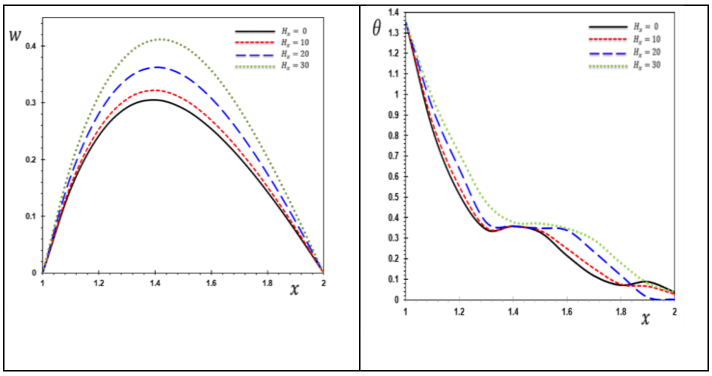

Figure 1: The variation of the deflection w with different values of initial magnetic field H_x.	**Figure 2**: The variation of temperature θ with different values of initial magnetic field H_x.

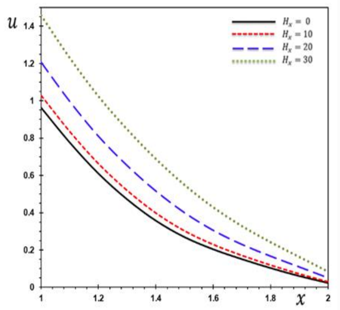

Figure 3: The variation of displacement u with different values of initial magnetic field H_x.

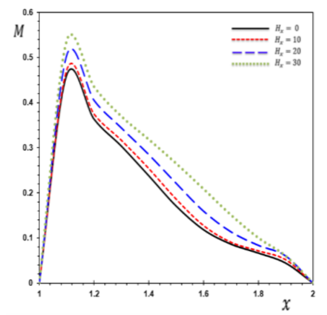

Figure 4: The variation of the flexure moment M with different values of initial magnetic field H_x.

6.2. The effect of Winkler and shear foundation parameters

In this section, particular attention is focused on the analytical and numerical analysis of Winkler and shear foundation parameters K_w and K_s on the beam response. To verify the influences of the Pasternak foundation parameters on the behavior of the microbeam, Figs. (5−8) are plotted. It is assumed that $K_w = K_s = 0$ for classical model (without foundation), $K_w = 100, K_s = 0$ for Winkler foundation model and $K_w = 100, K_s = 50$ or Pasternak foundation model. In all cases, the other parameters remain constant. From Fig.5 the deflection w reaches their highest values in the case $K_w = 0, K_s = 50$. Also we can observe that the deflection w has minimum values in the case of $(K_w = 100 , K_s = 0)$ compared with other cases. We observed as displayed in Fig. 6 the temperature θ in the case $K_w = K_s = 0$ is close to that in the case of $K_w = 100 , K_s = 0$.In Fig. 6 it noted that the displacement u in the case $K_w = K_s = 0$ is adjacent to that in the case of $K_w = 100 , K_s = 0$. Fig.8 shows that the flexure moment M in the absence of Pasternak $(K_w = 0 , K_s = 50)$ is less than the presence of Pasternak $(K_w = 100 , K_s = 50)$.

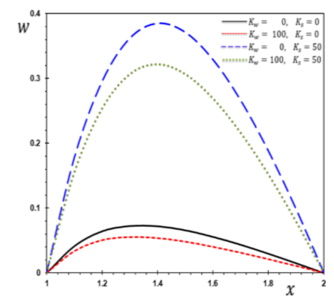

Figure 5: The deflection w with different Winkler and shear foundation parameters K_w and K_s

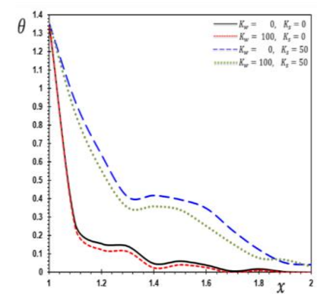

Figure 6: The temperature θ with different Winkler and shear foundation parameters K_w and K_s

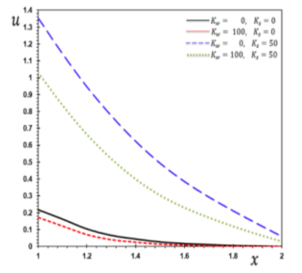

Figure 7: The displacement u with different Winkler and shear foundation parameters K_w and K_s

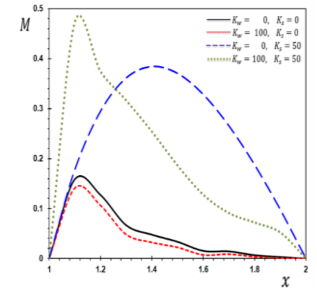

Figure 8: The flexure moment M with different Winkler and shear foundation parameters K_w and K_s.

6.3. The effect of the ramping time parameter t_0

This case investigates the influence of the ramping time parameter t_0 on the studied field quantities. Benchmark results are shown in Figs. 9−12 for future comparisons with other researchers. It is detected that the ramping time parameter t_0 has a pronounced effect on all the distribution of the physical fields. The variations are plotted vs the distance x for ramping time parameter t_0 when $K_w = 100, K_s = 50, \tau_\theta = 0.05, \tau_q = 0.03$ and $H_x = 10$.We can see that the values of the deflection w start decreasing with the ramping time parameter in the range $1 \le x \le 1.4$, thereafter increasing to maximum amplitudes in the range $1.4 \le x \le 2$ (see Fig. 9). From Fig. 10, we can conclude that the increase in the value of the ramping time parameter t_0 causes decreasing in the values of temperature θ . It is noted from Fig. 11 that the increase in the value of the ramping time parameter t_0 causes decreasing in the values of the displacement u which is very obvious in the peak points of the curves. As shown in Fig. 12 the values of the flexure moment M start decreasing with the ramping time parameter in the range $1 \le x \le 1.1$, there after increasing t_0 maximum amplitudes in the range $1.1 \le x \le 2$.

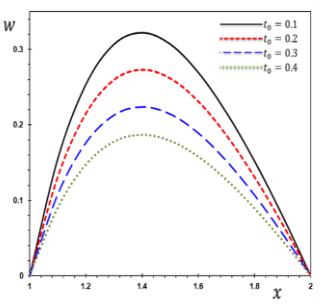

Figure 9: The deflection w with different ramping time

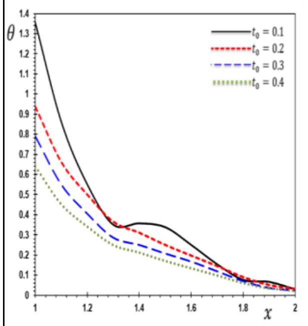

Figure 10: The temperature θ with different ramping time

parameter t_0.	parameter t_0.

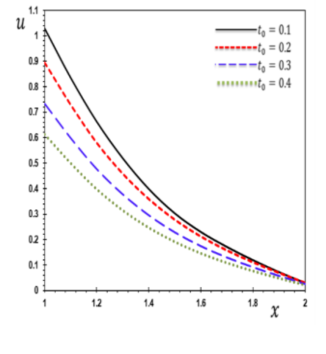

Figure 11: The displacement u with different ramping time parameter t_0.

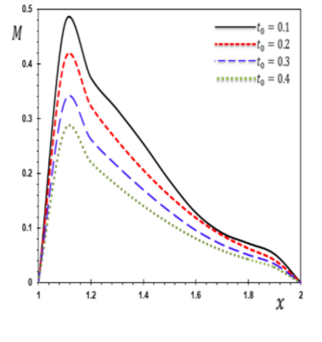

Figure 12: The flexure moment M with different ramping time parameter t_0.

6.4. Comparison between different models of thermoelasticity

The last case illustrates an important comparison between the different theories of thermoelasticity as they can be obtained as special cases from the presented model (DPL). The classical theory of thermoelasticity (CTE) can be obtained by setting $\tau_\theta = 0, \tau_q = 0$ and the generalized thermoelasticity with a single phase-lag (LS) can be achieved when $\tau_\theta = 0, \tau_q = 0.03$. The distributions of the deflection w, temperature θ, displacement u and the flexure moment M for different models of thermoelasticity are presented graphically in Figs. 13-16. The distribution in the LS model is near to that in the DPL model, but the distributions in the CTE model are different from those in the DPL model. From Fig. 13 we can observe that the deflection w reaches its maximum values in the case of DPL model compared with other theories. Fig.14 shows that the temperature distribution θ has a convergence between the different models of thermoelasticity. From Fig. 15 it is to be noted that the displacement u in the case of the LS model is close to that in the DPL model, while the displacement u in the CTE model is different from those in the DPL model. We observed also as displayed in Fig. 16 the distribution of the flexure moment M in the case of the LS model is small compared to the other models.

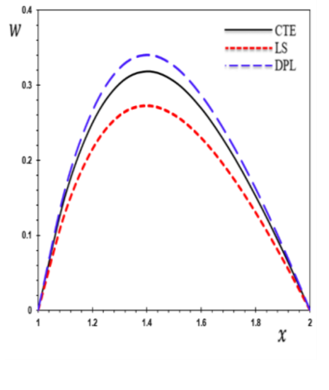

Figure 13: The deflection w in different models of thermoelasticity.

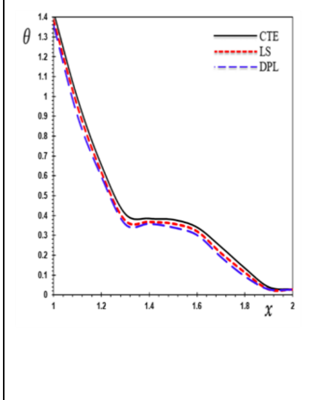

Figure 14: The variation of temperature θ in different models of thermoelasticity.

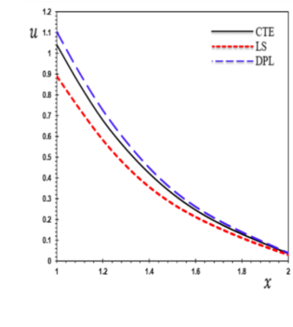

Figure 15: The variation of displacement u in different models of thermoelasticity.

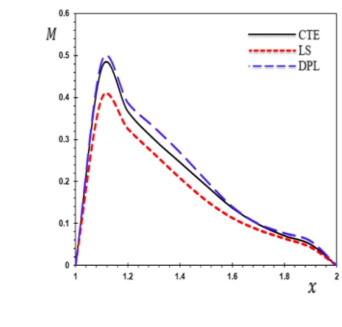

Figure 16: The variation of the flexure moment M in different models of thermoelasticity.

7. Conclusion

In this paper, we have analyzed the thermoelastic response of microbeams posted on a two-parameter viscoelastic foundation. One of these parameters represents the Winkler foundation parameter. The second parameter represents the shear foundation parameter. In this work, a new model of nonlocal generalized thermoelasticity based upon the Eringen theory for microbeams is constructed. The results are displayed graphically to explain the effect of the magnetic field, Winkler and shear foundation modulus, the ramping time parameter, and the models of thermoelasticity. The results indicate that the field quantities such as the deflection, temperature, displacement and the flexure moment of microbeam distributions depend not only on the space coordinate x but also depend on the magnetic field H_x, Winkler and shear foundation modulus K_w and K_s and the ramping time parameter t_0. The results of the present LS model are an agreement with those of the DPL model, whereas the results of the present CTE model are spaced with those of the DPL model. In this manuscript we can see a good agreement between the deviations obtained and those published. The results are useful for Microelectromechanical systems (MEMS) design and many other applications.

Nomenclature:

λ, μ	Lam´e's constants	K	thermal conductivity
α_t	thermal expansion coefficient	ρ	material density
C_E	specific heat	Q	heat source
$\gamma = (3\lambda + 2\mu)\,\alpha_t$	thermal coupling parameter	t	the time
T_0	environmental temperature	δ_{ij}	Kronecker's delta function
$\theta = T - T_0$	temperature increment	$\vec{E}$	induced electric field
T	absolute temperature	τ_q	phase lag of heat flux
$\mathbf{u}$	displacement vector	τ_θ	phase lag of temperature
$e = \mathrm{div}\,\mathbf{u}$	cubical dilatation	$\vec{J}$	current density
σ_{ij}	stress tensor	μ_0	magnetic permeability
e_{ij}	strain tensor	$\vec{h}$	induced magnetic field
q	heat flux vector	$\vec{H}$	magnetic field
M	the flexure moment	t_0	ramping time parameter
K_w	Winkler foundation parameter	K_s	shear foundation parameter
w	the deflection		

References

[1] B. Akgöz and Ö. Civalek, "Bending analysis of FG microbeams resting on Winkler elastic foundation via strain gradient elasticity," Composite Structures, vol. 134, pp. 294-301, 2015.

[2] H.-T. Thai, T. P. Vo, T.-K. Nguyen, and J. Lee, "Size-dependent behavior of functionally graded sandwich microbeams based on the modified couple stress theory," Composite Structures, vol. 123, pp. 337-349, 2015.

[3] B. Akgöz and Ö. Civalek, "Thermo-mechanical buckling behavior of functionally graded microbeams embedded in elastic medium," International Journal of Engineering Science, vol. 85, pp. 90-104, 2014.

[4] P. Belardinelli, M. Brocchini, L. Demeio, and S. Lenci, "Dynamical characteristics of an electrically actuated microbeam under the effects of squeeze-film and thermoelastic damping," International Journal of Engineering Science, vol. 69, pp. 16-32, 2013.

[5] M. Baghani, "Analytical study on size-dependent static pull-in voltage of microcantilevers using the modified couple stress theory," International Journal of Engineering Science, vol. 54, pp. 99-105, 2012.

[6] M. Pakdemirli and H. Boyacı, "Vibrations of a stretched beam with non-ideal boundary conditions," Mathematical and Computational Applications, vol. 6, pp. 217-220, 2001.

[7] M. Safarabadi, M. Mohammadi, A. Farajpour, and M. Goodarzi, "Effect of surface energy on the vibration analysis of rotating nanobeam," Journal of Solid Mechanics, vol. 7, pp. 299-311, 2015.

[8] M. Baghani, M. Mohammadi, and A. Farajpour, "Dynamic and stability analysis of the rotating nanobeam in a nonuniform magnetic field considering the surface energy," International Journal of Applied Mechanics, vol. 8, p. 1650048, 2016.

[9] M. Şimşek, "Nonlinear free vibration of a functionally graded nanobeam using nonlocal strain gradient theory and a novel Hamiltonian approach," International Journal of Engineering Science, vol. 105, pp. 12-27, 2016.

[10] M. H. Ghayesh, H. Farokhi, and M. Amabili, "Nonlinear dynamics of a microscale beam based on the modified couple stress theory," Composites Part B: Engineering, vol. 50, pp. 318-324, 2013.

[11] M. Caputo, "Linear models of dissipation whose Q is almost frequency independent—II," Geophysical Journal International, vol. 13, pp. 529-539, 1967.

[12] A. S. El-Karamany and M. A. Ezzat, "Convolutional variational principle, reciprocal and uniqueness theorems in linear fractional two-temperature thermoelasticity," Journal of Thermal Stresses, vol. 34, pp. 264-284, 2011.

[13] S. Pradhan and T. Murmu, "Thermo-mechanical vibration of FGM sandwich beam under variable elastic foundations using differential quadrature method," Journal of Sound and Vibration, vol. 321, pp. 342-362, 2009.

[14] M. Goodarzi, M. Mohammadi, M. Khooran, and F. Saadi, "Thermo-mechanical vibration analysis of FG circular and annular nanoplate based on the visco-pasternak foundation," Journal of Solid Mechanics, vol. 8, pp. 788-805, 2016.

[15] M. Mohammadi, M. Ghayour, and A. Farajpour, "Analysis of free vibration sector plate based on elastic medium by using new version of differential quadrature method," 2011.

[16] M. Mohammadi, A. Farajpour, M. Goodarzi, and H. Mohammadi, "Temperature effect on vibration analysis of annular graphene sheet embedded on visco-Pasternak foundation," Journal of Solid Mechanics, vol. 5, pp. 305-323, 2013.

[17] M. I. Younis, E. M. Abdel-Rahman, and A. Nayfeh, "A reduced-order model for electrically actuated microbeam-based MEMS," Journal of Microelectromechanical systems, vol. 12, pp. 672-680, 2003.

[18] A. Zenkour and M. Sobhy, "Dynamic bending response of thermoelastic functionally graded plates resting on elastic foundations," Aerospace Science and Technology, vol. 29, pp. 7-17, 2013.

[19] Y.-H. Chen, Y.-H. Huang, and C.-T. Shih, "Response of an infinite Timoshenko beam on a viscoelastic foundation to a harmonic moving load," Journal of Sound and Vibration, vol. 241, pp. 809-824, 2001.

[20] J. Abdalla and A. Ibrahim, "Development of a discrete Reissner–Mindlin element on Winkler foundation," Finite elements in analysis and design, vol. 42, pp. 740-748, 2006.

[21] R. Kumar, S. Kothari, and S. Mukhopadhyay, "Some theorems on generalized thermoelastic diffusion," Acta mechanica, vol. 217, pp. 287-296, 2011.

[22] D. Y. Tzou, "A unified field approach for heat conduction from macro-to micro-scales," 1995.

[23] D. Y. Tzou, Macro-to microscale heat transfer: the lagging behavior: John Wiley & Sons, 2014.

[24] M. A. Biot, "Thermoelasticity and irreversible thermodynamics," Journal of applied physics, vol. 27, pp. 240-253, 1956.

[25] H. Wang, K. Dong, F. Men, Y. Yan, and X. Wang, "Influences of longitudinal magnetic field on wave propagation in carbon nanotubes embedded in elastic matrix," Applied Mathematical Modelling, vol. 34, pp. 878-889, 2010.

[26] M. Hetenyi, "A general solution for the bending of beams on an elastic foundation of arbitrary continuity," Journal of Applied Physics, vol. 21, pp. 55-58, 1950.